Polymer 50 (2009) 4683–4689

Contents lists available at ScienceDirect

Polymer

journal homepage: www.elsevier.com/locate/polymer

Effect of crosslink density on fracture behavior of model epoxies containing block copolymer nanoparticles

Jia (Daniel) Liu [a], Hung-Jue Sue [a,*], Zachary J. Thompson [b], Frank S. Bates [b], Marv Dettloff [c], George Jacob [c], Nikhil Verghese [c], Ha Pham [c]

[a] Polymer Technology Center, Department of Mechanical Engineering, Texas A&M University, College Station, TX 77843, USA
[b] Department of Chemical Engineering and Materials Science, University of Minnesota, Minneapolis, MN 55455, USA
[c] The Dow Chemical Company, Epoxy R&D, Freeport, TX 77541, USA

ARTICLE INFO

Article history:
Received 1 March 2009
Received in revised form
27 April 2009
Accepted 2 May 2009
Available online 12 May 2009

Keywords:
Epoxy toughening
Block copolymer nanoparticle
Crosslink density

ABSTRACT

Model diglycidyl ether of bisphenol-A based epoxy resins containing well-dispersed 15 nm block copolymer (BCP) nanoparticles were prepared to study the effect of matrix crosslink density on their fracture behavior. The crosslink density of the model epoxies was varied *via* the controlled epoxy thermoset technology and estimated experimentally. As expected, it was found that the fracture toughness of the BCP-toughened epoxy is strongly influenced by the crosslink density of the epoxy matrix, with higher toughenability for lower crosslink density epoxies. Key operative toughening mechanisms of the above model BCP-toughened epoxies were found to be nanoparticle cavitation-induced matrix shear banding for the low crosslink density epoxies. The toughening effect from BCP nanoparticles was also compared with core-shell rubber-toughened epoxies having different levels of crosslink density. The usefulness of the present findings for designing toughened thermosetting materials with desirable properties is discussed.

1. Introduction

Rubber modification has been reported as an effective approach for toughening brittle epoxy thermosets since the beginning of the 1970s [1,2]. Since then, significant work has been done to gain a better understanding of the structure–property relationship between the polymer matrix and the toughening agents for designing epoxy thermoset systems with desired properties [3–19]. Self-assembled amphiphilic block copolymers (BCP) are a new type of toughening agent that has been shown to greatly improve toughness without sacrificing other mechanical properties. In our previous work [20,21] we identified the toughening mechanisms of a BCP-modified controlled epoxy thermoset (CET) system at a specific crosslink density. The major toughening mechanisms are BCP particle cavitation and subsequent matrix shear banding, which are analogous to those found in other rubber-toughened systems. But the BCP appears to be more effective than other conventional rubber particles, probably due to its much smaller sizes and unique morphology. In this paper we report the fracture behavior of BCP-toughened epoxy with variation in crosslink densities.

Although rubber modification has been recognized as an effective toughening approach, not all epoxy resins can be toughened to significant extents. *Toughenability* has been found to be related to thermoset crosslink density [22–30]. It is known that the crosslink density of a cured thermoset generally dictates its intrinsic ductility, simply because ductile deformation requires large-scale cooperative conformational arrangements of polymer backbones. Because matrix shear banding has been identified as the major energy dissipation process in rubber-toughened epoxies [5,6,9,11,20], it is not difficult to understand that modifying the matrix ductility can change its toughenability. The function of rubber particle cavitation is to relieve the triaxial stress at the crack tip and consequently to facilitate matrix shear banding. Thus, the thermoset matrix ductility plays an important role in enhancing fracture toughness of rubber-modified thermosets.

The present work is part of a larger effort to understand the fundamentals of structure–property relationships in a model epoxy system containing poly(ethylene-*alt*-propylene)-*b*-poly(ethylene oxide) (PEP-PEO) BCP nanoparticles. The toughening mechanisms and strain rate dependence of this modified epoxy system were reported earlier [20,21]. In this study, attention will be placed on determining whether or not the BCP-modified epoxy thermosets with variation in crosslink densities will exhibit a similar toughening effect on fracture behavior as what has been observed in

* Corresponding author. Tel.: +1 979 845 5024.
E-mail address: hjsue@tamu.edu (H.-J. Sue).

0032-3861/$ – see front matter © 2009 Elsevier Ltd. All rights reserved.
doi:10.1016/j.polymer.2009.05.006

Table 1
Chemical structures of epoxy resin, chain extender, crosslinker and block copolymer used in this investigation.

Product	Chemical structure
DGEBA epoxy resin	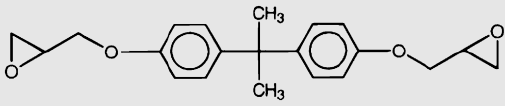
BPA chain extender	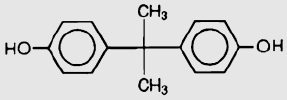
THPE crosslinker	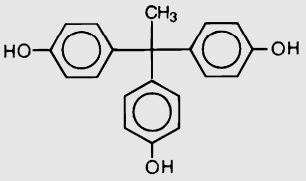
PEP-PEO block copolymer	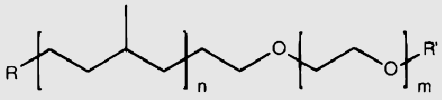

R = *s*-butyl or *t*-butyl
R′ = H or CH_3

other rubber-toughened systems. The implication of the present findings for designing high performance thermosetting resins is discussed in detail.

2. Experimental

2.1. Materials

The epoxy chemistry used for this study consisted of three components: diglycidyl ether of bisphenol-A (DGEBA)-based epoxy monomer (D.E.R.™ (Trademark of The Dow Chemical Company) 332, Dow Chemical), bisphenol-A (BPA) chain extender (PARABIS™ (Trademark of The Dow Chemical Company), Dow Chemical), and 1,1,1-tris(4-hydroxyphenyl)ethane crosslinker (THPE, Aldrich). The chemical structures of these reactants are given in Table 1.

A scheme of the chain extension and crosslinking reactions is illustrated in Fig. 1. The ratio of epoxy monomer and chain extender was altered to vary the crosslink density. The theoretical value of the molecular weight between crosslinks (M_c) was estimated by determining the average crosslink functionality (f_{cav}) and the average molecular weight per crosslinks (M_{pc}), assuming a balanced stoichiometry [31].

It is noted that ethyltriphenylphosphonium acetate (70% in methanol, Alfa Aesar) was utilized as a catalyst to promote reactions between primary epoxide groups in the epoxy resin and phenolic functionalities in the chain extender and the crosslinker. This largely reduced the chances of branching reactions with secondary hydroxyl groups and lead to a more uniform and controlled epoxy network.

As a toughing agent, the PEP-PEO amphiphilic BCP was synthesized using a multi-step polymerization method previously described by Hillmyer and Bates [32]. PEO is an epoxy-miscible block and PEP an epoxy-immiscible block, which forms a rubber domain with a size of about 15 nm. The number-average molecular weight (M_n) of the BCP is 9100 g/mol and the weight fraction of ethylene oxide in the BCP is 0.40. The chemical structure of PEP-PEO is also shown in Table 1.

2.2. Preparation of BCP-modified epoxy resin

The procedure for sample preparation has been reported in detail earlier [20], so it is only briefly described here. The BCP was mixed and completely dissolved in the epoxy resin at around 150 °C. Then, the chain extender and crosslinker were added into the mixture and dissolved. After degassing, the catalyst was added and the mixture was cured in a pre-heated mold for 2 h at 200 °C.

The BCP concentration in all final epoxy products was 5 wt%. Three crosslink densities of epoxy matrix were designed with theoretical M_c being 900, 1550 and 2870 g/mol, respectively. For convenience, the neat and modified epoxy samples with different M_c are designated as CET900, CET1550, CET2870, CET900/BCP, CET1550/BCP, and CET2870/BCP.

All the specimens were dried for at least 24 h in a vacuum oven set at 80 °C prior to characterizations.

2.3. Density measurement

The densities of all the samples were measured by the displacement method at room temperature following the ASTM

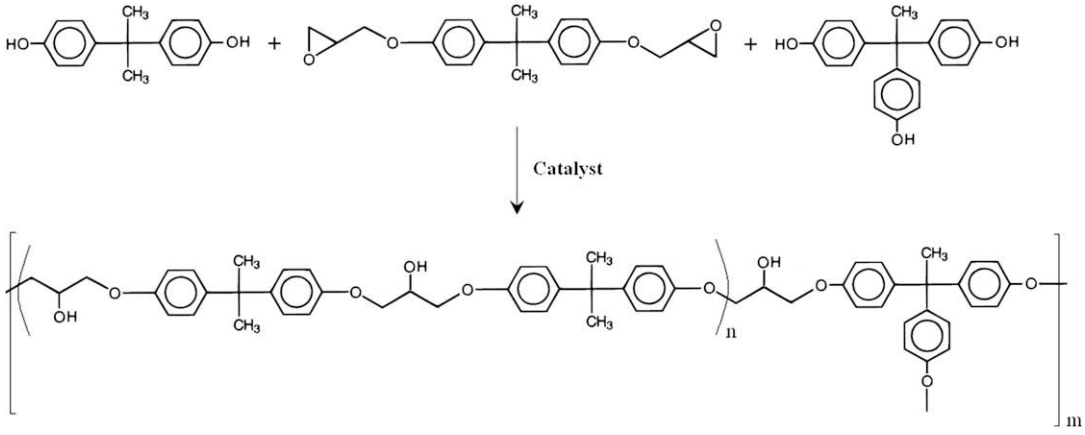

Fig. 1. Scheme of chain extension and crosslinking reactions in the present epoxy curing process.

D792-91 standard. Isopropyl alcohol, which has a known density of 0.785 g/cm^3, was used for immersion of the samples. The density was calculated using the equation:

$$\rho = \frac{W_a}{W_a - W_i}\rho_i \quad (1)$$

where W_a is the weight of the sample in air, W_i is the weight of the sample in isopropyl alcohol, and ρ_i is the density of isopropyl alcohol. To calculate the density at elevated temperatures, thermal mechanical analysis (TMA) was performed on a Q400 instrument (TA Instruments) to obtain the coefficient of thermal expansion (CTE) and to measure the dimensional change as the temperature increased.

2.4. Dynamic mechanical analysis (DMA)

DMA was performed using an RSA III instrument (TA Instruments) at temperatures ranging from −120 to 200 °C with a 5 °C per step increase. The tests were performed at a fixed frequency of 1 Hz. A sinusoidal strain–amplitude of 0.05% was chosen for the analysis. The dynamic storage modulus (E') and tan δ curves were plotted as a function of temperature. The temperature at the maximum in the tan δ curve was recorded as the T_g. The E' at 60 °C above T_g was chosen as the rubbery plateau modulus, E_r, for each system.

2.5. Fracture toughness measurement

To obtain the Mode-I critical stress intensity (K_{IC}) of the neat and modified epoxy samples, a single-edge-notch three-point-bending (SEN-3PB) test was performed using the linear elastic fracture mechanics (LEFM) approach in accordance with the ASTM D5045 standard. The dimensions of test specimens are 75 × 12.7 × 3.5 mm^3. A sharp pre-crack was generated in each sample by tapping with a fresh razor blade chilled with liquid N_2 and care was taken to make sure that the pre-crack exhibited a thumbnail-like shape crack front. The tests were done at room temperature on an MTS Insight machine. The testing crosshead speed was chosen as 0.508 mm/min. The K_{IC} was calculated using the following equation:

$$K_{IC} = \frac{P_C S}{BW^{3/2}} f(a/W) \quad (2)$$

where P_C is the load at crack initiation, S is the span width, B is the thickness of the specimen, a is the initial crack length, W is the width of the specimen, and $f(a/W)$ is the specimen geometry factor.

Average values and standard deviations of the K_{IC} were calculated on the basis of at least five specimens per sample.

2.6. Toughening mechanisms investigation

The double-notch four-point-bending (DN-4PB) technique was utilized to investigate the detailed toughening mechanisms of BCP-modified epoxy resins with various crosslink densities. The DN-4PB technique has been shown to be effective in probing micromechanical deformation mechanisms [10–14,16,17,20,21,29,33,34]. A detailed description of this technique can be found elsewhere [20]. The tests were conducted at a crosshead speed of 0.508 mm/min and at room temperature, on an MTS Insight machine. Thin-sections with a thickness of ca. 40 μm from the core region of the DN-4PB subcritical crack tip damage zone were obtained by sectioning and polishing, following the procedures described by Holik et al. [35]. Optical microscopy (OM) images were then taken under both bright field and cross-polarized field modes using an Olympus BX60 optical microscope. For transmission electron microscopy (TEM) observation, a block containing a subcritical crack tip damage zone was isolated from the specimen and embedded in an Epo-Fix embedding resin (Electron Microscopy Sciences). A detailed procedure for the preparation and staining of the samples can be found elsewhere [20]. TEM micrographs were taken from the stained sections using a JEOL 1200 EX electron microscope operated at an accelerating voltage of 100 kV.

3. Results and discussion

Previous TEM work [20] revealed that the BCP self-assembles into well-defined and well-dispersed spherical micelles with an average diameter of ca. 15 nm in CET1550/BCP. Because CET900/BCP and CET2870/BCP exhibit similar morphologies as CET1550/BCP, they are not shown here.

3.1. Dynamic mechanical behavior

The DMA curves of all the samples are compared in Fig. 2 and the E' and T_g values are listed in Table 2.

For the neat epoxies (Fig. 2a), as expected, T_g decreased with decreasing crosslink density, because T_g is prone to be affected by larger-scale molecular motions, which are directly related to the molecular weight between crosslinks for a thermoset system. However, by comparing the heights of the tan δ curves between the α-relaxation peak (T_g) and the β-relaxation peak, it shows that the higher M_c epoxy exhibits slightly lower damping characteristics.

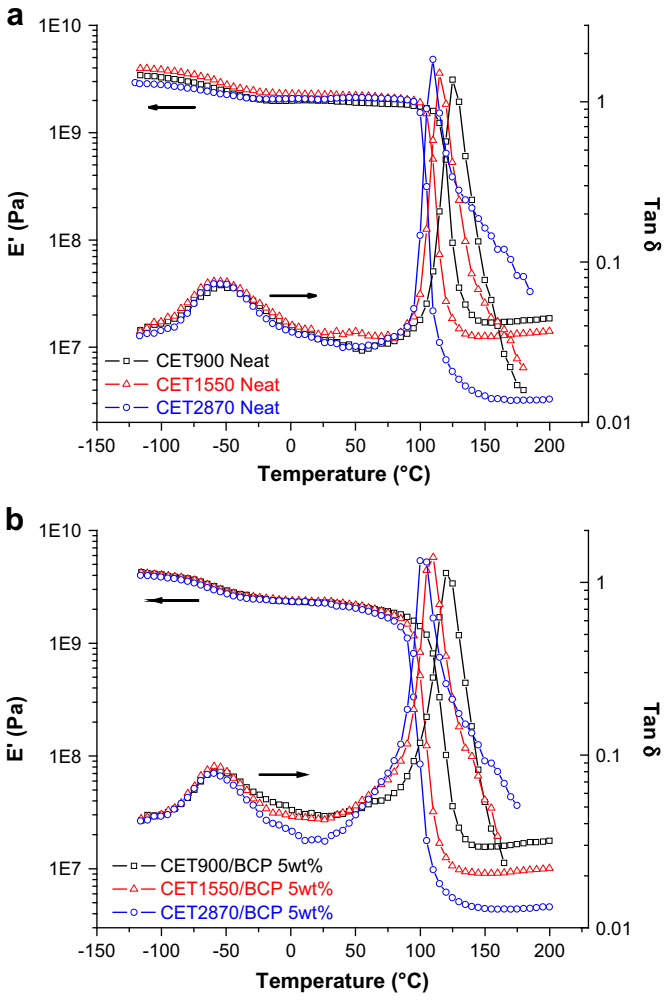

Fig. 2. DMA curves of (a) neat epoxies and (b) BCP-modified epoxies with different crosslink densities. The storage modulus (E') and glass transition temperature (T_g) values are summarized in Table 2.

Table 2
Storage modulus (E'), glass transition temperature (T_g) and fracture toughness (K_{IC}) of the samples.

Sample	E' (Pa)			T_g (°C)	K_{IC} (MPa m$^{1/2}$)
	At low temp.	At room temp.	At rubbery plateau		
CET900	3.27×10^9	1.99×10^9	1.79×10^7	125	0.82 ± 0.05
CET1550	3.86×10^9	2.25×10^9	1.33×10^7	115	0.96 ± 0.04
CET2870	2.80×10^9	2.04×10^9	3.20×10^6	110	0.94 ± 0.03
CET900/BCP	4.07×10^9	2.31×10^9	1.68×10^7	120	1.95 ± 0.03
CET1550/BCP	4.04×10^9	2.36×10^9	9.38×10^6	110	2.73 ± 0.08
CET2870/BCP	3.87×10^9	2.27×10^9	4.38×10^6	100	3.02 ± 0.17

Following this logic, the higher crosslink density epoxy should be more capable of dissipating fracture energy (tougher), which was found not to be the case (see Section 3.3). This observation further implies that the toughenability of epoxies cannot be simply correlated with the magnitude of tan δ curve from DMA alone. The physical nature responsible for the observed damping phenomenon is much more important for the correlation with toughenability. To be noted, the above finding has also been found in a core-shell rubber (CSR)-modified epoxy system [29].

As will be discussed in detail in the next section, the rubbery plateau modulus is inversely related to the M_c. But it is much more complex for storage moduli at low and ambient temperatures. The CET1550 has a higher E' than those of CET900 and CET2870. It is known that modulus is influenced more by the localized small-scale molecular motions, backbone rigidity, or chain rotation. Therefore, with the addition of more chain extender between crosslinks, there is likely to be a competition between a decrease in crosslink density and an increase in backbone rigidity, because the BPA chain is more rigid than the diglycidyl ether segment in the epoxy monomer.

For BCP-toughened epoxies (see Fig. 2b), the general crosslink density effects on storage modulus, T_g and damping curve are analogous to those of their neat epoxy counterparts. It is worth mentioning that there is a consistent increase in room temperature storage modulus for all BCP-containing epoxy samples relative to their neat controls. This finding indicates that the modulus of the epoxy is not compromised with the incorporation of BCP toughening agent, as has been reported earlier [20,21].

3.2. Determination of crosslink density

As stated earlier, the theoretical value of M_c was calculated from the stoichiometry of epoxy resin, chain extender and crosslinker. The crosslink density of each sample was also experimentally estimated by measuring the equilibrium storage modulus in the rubbery state, according to the equation from the theory of rubber elasticity [36]:

Table 3
Density and molecular weight between crosslinks (M_c) of the model epoxy systems.

Sample	Density at room temp. (g/cm^3)	Density at rubbery plateau (g/cm^3)	Theoretically estimated M_c (g/mol)	Experimentally estimated M_c (g/mol)
CET900	1.212	1.127	900	320
CET1550	1.200	1.127	1550	950
CET2870	1.204	1.133	2870	3890
CET900/BCP	1.204	1.117	–	750
CET1550/BCP	1.200	1.127	–	1320
CET2870/BCP	1.201	1.117	–	2760

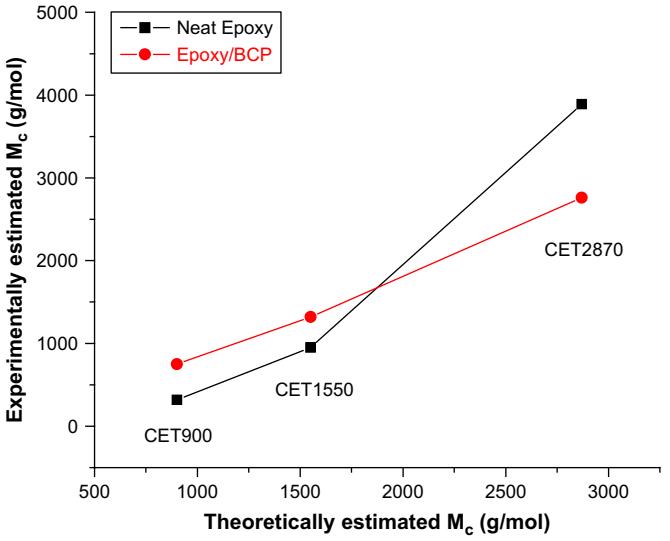

Fig. 3. Correlations of theoretical M_c and experimental M_c estimated using the rubber elasticity equation for the neat and modified epoxies in this study.

$$M_c = \frac{\rho RT}{G_r} \tag{3}$$

where ρ (in g/m^3) is the density of the polymer, G_r (in Pa) the shear equilibrium storage modulus in the rubbery state, M_c in g/mol and R and T are the real gas constant (8.314 J/K mol) and temperature (in Kelvin), respectively. The density of each sample at room temperature was first measured by the displacement method. The density in the rubbery state was calculated on the basis of the dimensional change from the CTE information obtained from TMA (the density data are given in Table 3). The G_r value is assumed to be related to the flexural equilibrium storage modulus, E_r, in the following manner:

$$E_r = 2G_r(1+\nu) \tag{4}$$

where ν is the Poisson's ratio and assumed to be 0.5 which is typical for a rubbery material. E_r was obtained from DMA at rubber plateau region (see Table 2).

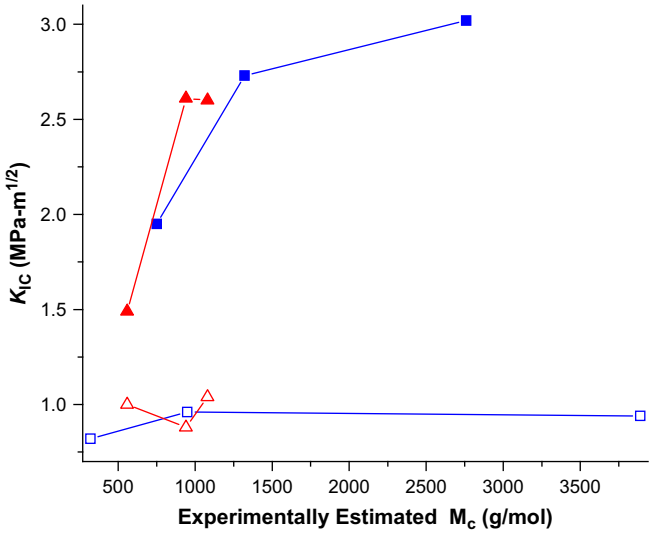

Fig. 4. Fracture toughness, K_{IC}, plotted against the matrix M_c for two sets of neat and modified epoxy resins: the ones in the present work (□ unmodified and ■ 5 wt% BCP-modified) and in Ref. [29] (△ unmodified and ▲ 5 wt% CSR-modified). The experimental estimated M_c data of the CSR system were reprocessed using Eq. (3) from the rubber elasticity theory.

For convenience, the theoretically and experimentally determined M_c values of all the samples in this study are listed in Table 3. As expected, there is a discrepancy between the experimentally determined M_c and the expected theoretical value of M_c, but the correlation between the experimental and theoretical M_c values follows a linear trend except for the neat CET2870 sample (Fig. 3). We also tried to estimate M_c using other means [37,38]. All gave similar trends but different numbers. Here, the simplest form of estimation, i.e., Eq. (3), was chosen for this study. It is noted that the cured epoxy network is far more complex than that of an ideal rubber. The estimated M_c values here are only meant to provide a semi-quantitative assessment of the crosslink density of the epoxy network investigated. To make the comparison meaningful, all the M_c values reported in this study, including those obtained from literature, were calculated using Eq. (3).

It is interesting to note that the presence of the BCP seems to lower the crosslink density of the epoxy matrix for CET900 and CET1550 systems. There is no evidence of any chemical reaction between the BCP and epoxy components. It is believed that the major interaction between the two phases is through hydrogen bonding between the –OH groups generated during the cure reaction and the ether oxygen in the PEO backbone [21]. The presence of the BCP phase, especially the epoxy-philic PEO block may somehow hinder the crosslinking process. This is possibly the explanation for the observed increase in M_c with the addition of BCP. The BCP effect on crosslink density may partially account for the altered matrix toughenability and the high strain rate sensitivity [21], as well. This effect was not observed for the lightly crosslinked CET2870 system.

3.3. Fracture toughness measurement

The fracture toughness values of the neat epoxies and the BCP-modified epoxies with various M_c are summarized in Table 2. It is evident that the addition of the BCP with an overall concentration of only 5 wt% can significantly improve the fracture toughness at all crosslink densities. As expected, the fracture toughness of the BCP-modified epoxies is strongly dependent on the matrix crosslink density. The higher the epoxy M_c, the higher the K_{IC} value becomes. Such a crosslink density effect is not found in the neat system. The matrix M_c does not seem to have much influence on the fracture toughness of the neat epoxies. By comparing the relative K_{IC}

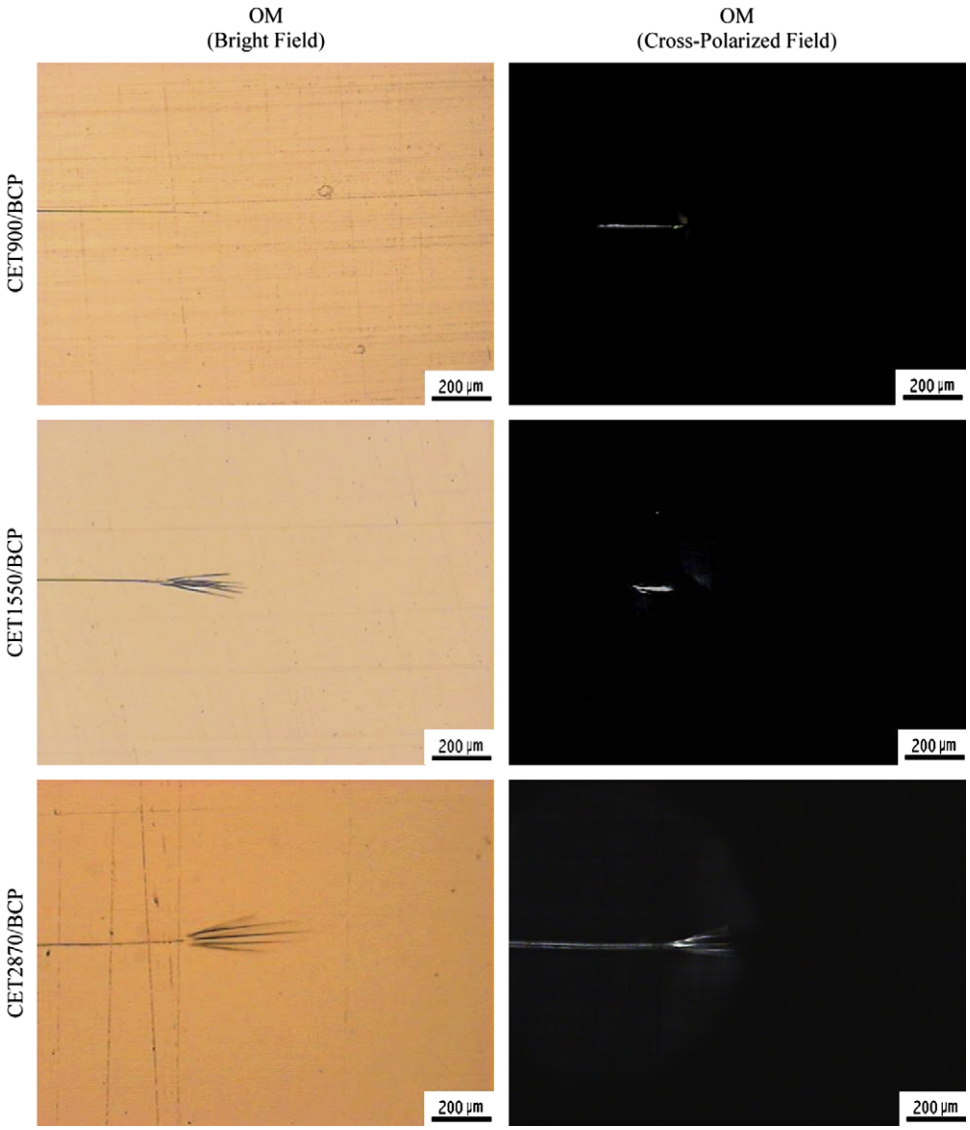

Fig. 5. OM images of subcritical crack tip regions in CET900/BCP, CET1550/BCP and CET2870/BCP, respectively. All the cracks propagate from left to right. The images were taken under both bright and cross-polarized fields at same location for each example.

improvement in each M_c case, it is not difficult to find that the lower crosslink density epoxy has a higher capability of being toughened through the incorporation of BCP toughening agent, i.e., a higher *toughenability*.

In addition, the above crosslink density–toughenability correlation has been compared with that in a 5 wt% CSR-modified epoxy system [29], as shown in Fig. 4. The CSR particle has a butadiene–styrene core (84 wt%) and a styrene–methylmethacrylate–acrylonitrile–glycidylmethacrylate shell (16 wt%) and has an average diameter of ca. 120 nm. The comparison of toughening effect between the two rubber tougheners suggests that the BCP phase is at least as effective as CSR in toughening epoxies of various crosslink densities. In addition, there appears to be a critical M_c value for the rubber-modified systems beyond which the further enhancement in fracture toughness will diminish. The above phenomenon may be due to the fact that the high M_c rubber-toughened epoxy is too tough for the LEFM approach to become valid. The *J*-integral approach has to be undertaken to account for the high toughening effect of the high M_c epoxy resins.

3.4. Crosslink density effect on toughening mechanisms

As aforementioned, it is imperative to investigate the physical nature and micromechanical mechanisms of the toughening process for a fundamental understanding of crosslink density effect. With the aid of the DN-4PN technique, the key toughening mechanism in these modified epoxies has been found to be BCP nanoparticle cavitation-induced matrix shear banding [20]. This study focuses on the difference in major toughening effects from the influence of the matrix crosslink density.

Fig. 5 presents the OM images of the subcritical crack tip damage zones in the modified epoxies after the DN-4PB test under both bright field and cross-polars. It is clear from the bright field images that, the lower the crosslink density, the larger the damage zone size that is formed in front of the crack tip. In the images taken under cross-polarized light, a birefringent zone is observed in the middle of the crack tip damage zone, indicating a shear banding process. It is also found that the size and the intensity of the shear banding zone increase with decreasing crosslink density.

To understand the details of the micromechanical deformation process upon fracture, TEM was performed to examine the specific location in the vicinity of the subcritical crack tips in the BCP-modified epoxies after DN-4PB (Fig. 6). In the case of CET900/BCP, some cavitated nanoparticles have been found to remain spherical in shape, even in the regions immediately beneath the crack path. As for CET1550/BCP, the cavitation phenomenon becomes more uniform, and some form of stretching and orientation of the BCP nanoparticles has been found, which indicates the shear plastic deformation of the matrix around those particles. The micromechanical mechanisms found in the case of CET2870/BCP are similar to CET1550/BCP, but the degree of particle deformation is more pronounced. As indicated in the TEM micrograph, cavitated BCP particles adjacent to the crack seem to have undergone severe stretching.

All the information obtained from OM and TEM observations is consistent with the fracture toughness results. It is evident that the particle cavitation and matrix shear banding mechanisms are highly suppressed for high crosslink density epoxies. The higher the M_c the more flexible the network architecture becomes. This means it is more likely that the material can undergo plastic deformation and dissipate more fracture energy through intermolecular motions.

It is known that normally epoxy itself is extremely difficult to have shear deformation under high triaxial stress state (plane-strain condition), e.g., at the crack tip. Thus, the effect on the energy dissipation process above M_c has to be with the presence of rubbery particles, because cavitation of those particles can relieve the local

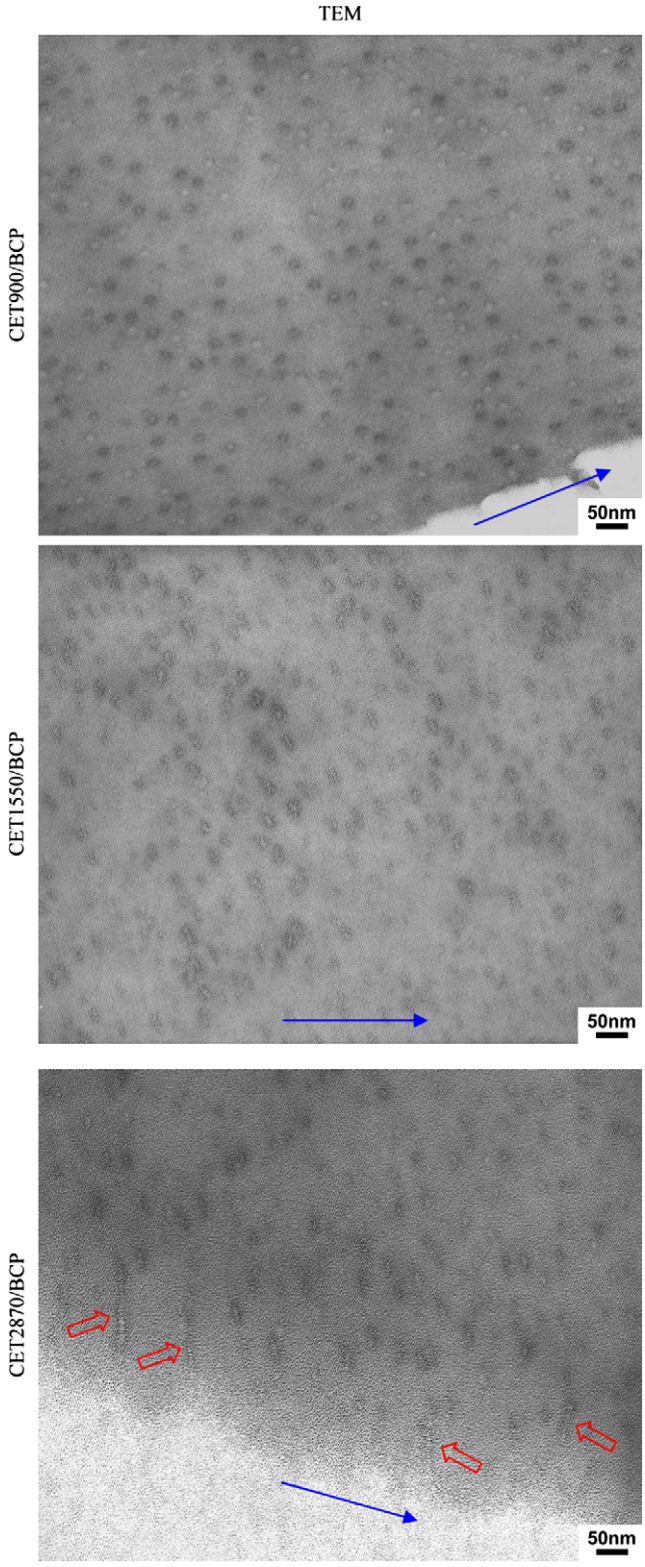

Fig. 6. TEM micrographs taken in the vicinity of subcritical crack tips in CET900/BCP, CET1550/BCP and CET2870/BCP, respectively. The specimen thin-sections were stained using 0.5% RuO_4 aqueous solution prior to TEM imaging. The crack propagating directions are indicated in the images. In the CET2870/BCP image, the arrows point to the BCP nanoparticles that are severely stretched.

triaxial stress and alter the stress state to plane-stress condition. That is also why the crosslink density effect seems to be a nonfactor in neat thermosetting systems. On the other hand, a sufficiently high ductility matrix is considered a fundamental requirement for a thermosetting material to be toughenable by the incorporation of rubbery phase.

It is worth mentioning that the correlation between crosslink density and toughenability may not necessarily hold true when the nature of epoxy backbone molecular rigidity or the applied stress state is altered. Sue et al. have found a totally opposite M_c–toughenability relationship in two toughened epoxy resins with different side groups on the epoxy monomers [29]. The toughenability of an epoxy resin has also been altered by Kishi et al. by changing the stress state [28] or the shear ductility through the incorporation of ductile thermoplastic resins [27].

3.5. Implications of the present work

Generally speaking, in rubber-toughened polymeric systems, the properties of the elastomeric phase, such as cavitational strength, particle size, concentration, etc., are critical for the resulting toughening effect. Also, the nature of the matrix definitely plays an important role in determining whether or not toughening mechanisms can operate effectively. The crosslink density in thermosetting materials is one example. Although a crosslink density–toughenability relationship has been clearly revealed with experimental evidence in this study, the questions as to how the epoxy network develops during curing and how that process can be influenced by the presence of a heterogeneous inclusion, still remain unanswered. There is also no direct technique that can definitively probe the inhomogeneity, unreacted functionality, or other defects in a thermosetting resin. More efforts are still needed to achieve a complete understanding of structure–property relationship of engineered thermosets at the molecular level.

4. Conclusions

The fracture characteristics of PEP-PEO BCP-modified epoxies were carefully studied with variations in matrix crosslink density. As expected, the findings suggest that the toughenability of the epoxy resin has a strong dependence on its M_c. The lower the crosslink density is, the more capable the host resin can be toughened by the incorporation of the elastomeric phase. The nano-sized BCP particles appear to be at least as effective as CSR in toughening epoxies at various levels of crosslink densities. It is possible to develop a high performance thermosetting material with combined desirable T_g, modulus and toughenability. Additional work is still needed for understanding the physical nature of network formation and its interactions with BCP particles at nanometer scale, especially at their interphase.

Acknowledgments

The authors would like to gratefully acknowledge the funding supports from The Dow Chemical Company and the Department of Energy (DOE) through grant 5–35908 and through a subcontract to UT–Battelle (No. 4000041622) for the current research.

References

[1] Sultan JN, Liable RC, McGarry FJ. Polym Symp 1971;16:127.
[2] Sultan JN, McGarry FJ. J Polym Eng Sci 1973;13:29.
[3] Kinloch AJ, Shaw SJ, Tod DA, Hunston DL. Polymer 1983;24:1341.
[4] Kinloch AJ, Shaw SJ, Hunston DL. Polymer 1983;24:1355.
[5] Yee AF, Pearson RA. J Mater Sci 1986;21:2462.
[6] Pearson RA, Yee AF. J Mater Sci 1986;21:2475.
[7] Garg AC, Mai Y-W. Compos Sci Technol 1988;31:179.
[8] Garg AC, Mai Y-W. Compos Sci Technol 1988;31:225.
[9] Pearson RA, Yee AF. J Mater Sci 1991;26:3828.
[10] Sue H-J. Polym Eng Sci 1991;31:270.
[11] Sue H-J. Polym Eng Sci 1991;31:275.
[12] Sue H-J, Pearson RA, Yee AF. Polym Eng Sci 1991;31:793.
[13] Sue H-J. J Mater Sci 1992;27:3098.
[14] Sue H-J, Garcia-Meitin EI, Orchard NA. J Polym Sci Part B Polym Phys 1993;31:595.
[15] Kinloch AJ, Yuen ML, Jenkins SD. J Mater Sci 1994;29:3781.
[16] Sue H-J, Yee AF. Polym Eng Sci 1996;36:2320.
[17] Sue H-J, Garcia-Meitin EI, Pickelman DM, Bott CJ. Colloid Polym Sci 1996;274:342.
[18] Groleau MR, Shi YB, Yee AF, Bertram JL, Sue H-J, Yang PC. Compos Sci Technol 1996;56:1223.
[19] Derkowski BJ, Sue H-J. Polym Compos 2003;24:158.
[20] Liu J, Sue H-J, Thompson ZJ, Bates FS, Dettloff M, Jacob G, et al. Macromolecules 2008;41:7616.
[21] Liu J, Sue H-J, Thompson ZJ, Bates FS, Dettloff M, Jacob G, et al. Acta Mater 2009;57:2691.
[22] Pearson RA, Yee AF. J Mater Sci 1989;24:2571.
[23] Iijima T, Yoshioka N, Tomoi M. Eur Polym J 1992;28:573.
[24] Iijima T, Miura S, Fukuda W, Tomoi M. Eur Polym J 1993;29:1103.
[25] Lu F, Plummer CJG, Cantwell WJ, Kausch HH. Polym Bull 1996;37:399.
[26] Lu F, Kausch HH, Cantwell WJ, Fischer MJ. Mater Sci Lett 1996;15:1018.
[27] Kishi H, Shi YB, Huang J, Yee AF. J Mater Sci 1997;32:761.
[28] Kishi H, Shi YB, Huang J, Yee AF. J Mater Sci 1998;33:3479.
[29] Sue H-J, Puckett PM, Bertram JL, Walker LL, Garcia-Meitin EI. J Polym Sci Part B Polym Phys 1999;37:2137.
[30] Kang BU, Jho JY, Kim JK, Lee SS, Park M, Lim S, et al. J Appl Polym Sci 2001;79:38.
[31] Lesser AJ, Crawford EJ. Appl Polym Sci 1997;66:387.
[32] Hillmyer MA, Bates FS. Macromolecules 1996;29:6994.
[33] Sue HJ, Bertram JL, Garcia-Meitin EI, Wilchester JW, Walker LL. Colloid Polym Sci 1994;272:456.
[34] Sue H-J, Puckett PM, Garcia-Meitin EI, Bertram JL. J Polym Sci Part B Polym Phys 1995;33:2003.
[35] Holik AS, Kambour RP, Hobbs SY, Fink DG. Microstruct Sci 1979;7:357.
[36] Ferry JD. Viscoelastic properties of polymers. 3rd ed. New York: John Wiley & Sons; 1980.
[37] Nielsen LE. J Macromol Sci 1969;C3:69.
[38] Timm DC, Ayorinde AJ, Foral RF. Br Polym J 1985;17:227.